Binary Root Protograph LDPC Codes for CSK Modulation to Increase the Data Rate and Reduce the TTD

Lorenzo Ortega Espluga, *TéSA*, Toulouse, France.
Charly Poulliat, *University of Toulouse, INPT, ENSEEIHT*, Toulouse, France
Marie-Laure Boucheret, *University of Toulouse, INPT, ENSEEIHT*, Toulouse, France
Marion Aubault-Roudier, *CNES*, Toulouse, France
Hanaa Al-Bitar, *Thales Alenia Space*, Toulouse, France

BIOGRAPHIES

Lorenzo Ortega received the Eng. degree in Telecommunication Engineering in 2014, and the M.Sc degree in Telecommunication and Signal Processing in 2016, both from Zaragoza University. In 2016, he coursed the second year of International Master of Electronics Systems for Embedded and Communicating Applications at the INP-ENSEEIHT (University of Toulouse) as an exchange student. Currently he is a PhD student at ENSEEIHT (University of Toulouse) and studies methodologies to optimize the signal structure of the new generation of Galileo. His thesis is funded by CNES (French Space Agency) and Thales Alenia Space.

Charly Poulliat received the Eng. degree in Electrical Engineering from ENSEA, Cergy-Pontoise, France, and the M.Sc. degree in Signal and Image Processing from the University of Cergy-Pontoise, both in June 2001. From Sept. 2001 to October 2004, he was a PhD student at ENSEA/University Of Cergy-Pontoise/CNRS and received the Ph.D. degree in Signal Processing for Digital Communications from the University of Cergy-Pontoise. From 2004 to 2005, he was a post-doctoral researcher at UH coding group, University of Hawaii at Manoa. In 2005, he joined the Signal and Telecommunications department of the engineering school ENSEA as an Assistant Professor. He obtained the habilitation degree (HDR) from the University of Cergy-Pontoise in 2010. Since Sept. 2011, he has been a full Professor with the National Polytechnic Institute of Toulouse (University of Toulouse, INP-ENSEEIHT). His research interests are signal processing for digital communications, error control coding and resource allocation.

Marie-Laure Boucheret received the Eng. degree in Electrical Engineering from ENST Bretagne, Toulouse, France, and the M.Sc. degree in Signal Processing from the University of Rennes, both in June 1985. In June 1997, she received the Ph.D. degree in Communications from TELECOM ParisTech, and the "Habilitation Ãă diriger les recherches" in June 1999 from INPT University of Toulouse. From 1985 to 1986 she has been a research engineer at the French Philips Research Laboratory (LEP). From 1986 to 1991, she has been an engineer at Thales Alenia Space, first as a project engineer (TELECOM II program) then as a study engineer at the transmission laboratory. From 1991 to 2005 she was a Associated Professor then a Professor at TELECOM ParisTech. Since March 2005 Marie-Laure Boucheret is a Professor at the National Polytechnic Institute of Toulouse (ENSEEIHT - University of Toulouse). She is also with the Signal and Communication group of the IRIT Laboratory.

Aubault-Roudier is a radionavigation engineer in the navigation/location signals department in CNES, the French Space Agency, where she is involved in the optimization of GNSS signals. Marion Aubault-Roudier graduated as an electronics engineer in 2011 from ENAC (Ecole Nationale de lâĂŹAviation Civile) in Toulouse, France. She received her PhD in 2015 from the Department of Mathematics, Computer Science and Telecommunications of the INPT (Polytechnic National Institute of Toulouse), France.

Hanaa Al-Bitar is a GNSS systems engineer at Thales Alenia Space France. She received her Ph.D in RadioNavigation in 2007 form the ENAC, in Toulouse, France, in the field of GNSS receivers. She joined TAS-F in 2012. Her main activities focus on GNSS signal processing, and SBAS Land Earth Stations signal processing and design.

ABSTRACT

New generation of GNSS systems seeks to provide new features in order to create or to improve their currents services. Between those possible features; the increase of the data rate is necessary in order to to provide services such as authentication, precise positioning or reduce the Time-To-First-Fix (TTFF). On the other hand, the data availability in harsh environment suggest the need of error correcting technologies. Then, based on previous works over the Code-Shift Keying (CSK) modulation and in Root Protograph LDPC code to reduce the TTFF, in this paper, it is presented the optimization of Root Protograph LDPC codes for the CSK modulation in a Bit-Interleaved Coded Modulation context and the optimization of Root Protograph LDPC codes for the CSK modulation in Bit-Interleaved Coded Modulation Iterative Decoding context. Both optimization where base on the Protograph EXIT chat algorithm, providing promising results.

I-INTRODUCTION

In the current state of the Global Navigation Satellite Systems (GNSS), the increase of the data rate is necessary in order to provide new features such as reduction of the Time-To-First-Fix (TTFF), authentication, integrity or precise positioning. Moreover, the data availability in hostile environments such as urban or jamming environments point out the need for using error correction mechanisms.

In previous works, the Code-Shift Keying (CSK) modulation has been chosen as an alternative to current Binary Phase-Shift Keying (BPSK) since it allows for an increase of the data rate and it enables non-coherent demodulation [5]. Additionally, modern channel coding techniques were specifically designed for the CSK modulation in order to design optimal codes which reduce the frame error probability. Indeed, in [13], an irregular binary Low Density Parity Check (LDPC) code of ratio 1/2 for a CSK modulation in a Bit Interleaved Coded Modulation (BICM) [3] context has been optimized. To compute the optimal irregular LDPC code distributions, an asymptotic analysis has been firstly done via EXtrinsic Information Transfer (EXIT) charts [16] in an Additive White Gaussian Noise (AWGN) propagation channel, to show that bit interleaved iterative decoding for a CSK modulated signal (consisting in adding a soft feedback between the LDPC decoder and the soft CSK demodulator) can significantly outperform non-iterative decoding. Based on this analysis, an asymptotic optimization is performed in order to design the LDPC code profiles [13], for a CSK-modulated signal, in an AWGN propagation channel and for iterative decoding. From these results, finite length parity-check matrices were generated thanks to the Progressive Edge Growth (PEG) algorithm [14].

Futhermore, in previous works [10] [9] the Root Codes [2] were proposed in the GNSS domain as coding alternative to reduce the TTFF. These codes are characterized by the Maximum Distance Separable (MDS) [11] property which allows to reduce the Time To Data (TTD) [11] [15] under good channel conditions. Moreover, these codes are full diversity under the Belief Propagation (BP) algorithm [2], which means that they have good error correction capabilities under harsh environments. Furthermore, the Root codes can be represented by a Protograph [18] representation [12] [4]. A Protograph can be represented using a Tanner graph $G = (N, M, E)$ for which parallel edges are permitted. An LDPC code is obtained from this Protograph by "lifting", ie. using a graph expansion based on circulant matrices [18]. The resulting structured codes are characterized by their excellent error correction capabilities and their ability to enable fast encoding and efficient decoding.

Considering the precedent in this article, we propose the two following schemes to increase the data rate and reduce the TTD :

- Bit-Interleaved Coded Modulation (BICM): A Protograph Root binary LDPC code of rate 1/2 for non-iterative decoding. In order to compute an optimal Root Protograph binary LDPC code distribution for the BICM scheme, an approach of the the Protograph EXIT (PEXIT) chart algorithm proposed in [8] is used to minimizing the demodulation threshold.
- Bit-Interleaved Coded Modulation Iterative Decoding (BICM-ID): Based on bit interleaved iterative decoding between the LDPC decoder and the soft in put soft output CSK demodulator, we propose a Protograph Root binary LDPC code of rate 1/2. In order to compute an optimal Root Protograph binary LDPC code distribution for the BICM-ID scheme, again we used an approach of the Protograph EXIT (PEXIT) chart algorithm, where it is included the EXIT chart information from the soft input soft output CSK demodulation in an AWGN propagation channel and under the iterative decoding assumption.

This paper is divided as follows: In section II, the fundamental of the CSK modulation as well as the log-likelihood ratio (LLR) expression derivation are presented. In section III, the Root Protograph LDPC codes are presented.

In section IV, we present the optimization method based on the PEXIT Charts for a CSK modulated signal in an AWGN channel for the BICM scheme and in section V, we present the optimization method based on the PEXIT Charts for a CSK modulated signal in an AWGN channel for the BICM-ID scheme. Results are presented in section VI. Conclusions are finally drawn in section VII.

II-CSK SYSTEM MODEL AND LLR EXPRESSION DERIVATION

The code shift keying (CSK) modulation [19] is an M-ary orthogonal modulation which was first proposed as a GNSS signal candidate in [5]. Each symbol x_l, corresponds with a different circular shift of a single unique PRN sequence c. Let $S_L = l, 1 \leq l \leq 2^k = M$ be the set of data symbols, with k the number of bits to be sent, then the PRN sequence c_l associated to the symbol $x_l, l \in S_L$, satisfies the following rule:

$$c_l(i) = c(mod(i - m_l, N)), \forall l \in [1, 2^k], \forall i \in [1, N] \tag{1}$$

where m_l is the integer number corresponding to the shift of the lth symbol, N is the number of chips in the PRN sequence and $mod(x, y)$ is the modulus operation.

As an example, in figure 1, it is illustrated the PRN sequences associated to the 4-ary CSK modulation with $N = 10230$ chips.

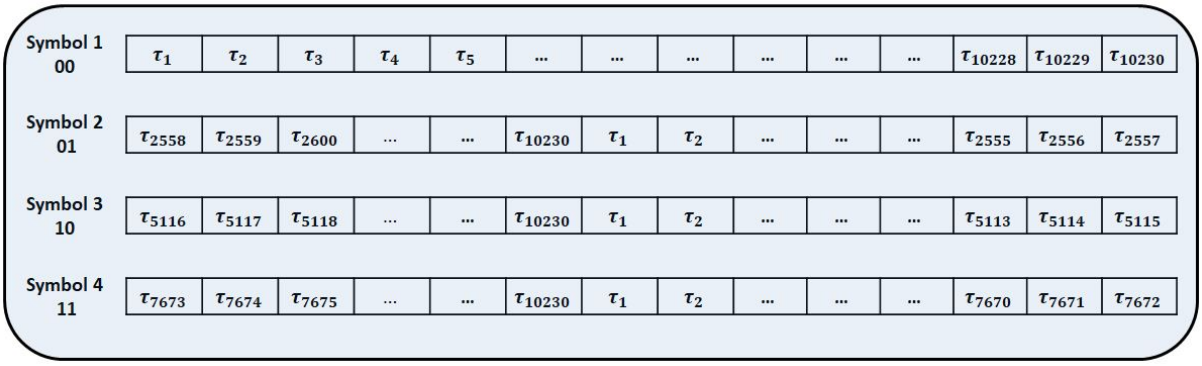

Figure 1: CSK Symbol Waveform Example

At the transmitter, the bits are encoded by the Root Protograph code to generate the codeword. Then, the codeword bits are grouped into a vector of k bits, generating a CSK symbol x_l. After that, the M-ary CSK associates each symbol x_l to an appropriated PRN sequence c_l by right shifting the fundamental PRN sequence c.

Log-Likelihood Ratio Computation

Now, let's denote $X = c_l$ the transmitted CSK PRN sequence associated to the vector sequence $[b_1, b_2, \ldots, b_k]$ and the CSK symbol x_l, and $Y = y_l$ the received sequence corresponding to X. Assuming AWGN channel:

$$y_l = c_l + n_l \tag{2}$$

where $n_l \sim \mathcal{N}(0, \sigma^2)$ are the centered $i.i.d.$ Gaussian noise samples with variance $\sigma^2 = N_0/2$.

Then, considering perfect synchronization, the a posteriori probability (APP) of the qth bit of the emitted CSK PRN sequence X can be represented by APP log likelihood ratio (LLR) expression of the bit:

$$LLR_{APP_q} = \log\left(\frac{P(b_q = 1|Y)}{P(b_q = 0|Y)}\right) \tag{3}$$

where $P(b_q = 1|Y)$ and $P(b_q = 0|Y)$ represent the probability that $b_q = 1$ and $b_q = 0$, respectively, considering the received sequence Y.

Considering the Bayer's rule, equation (3) yields to:

$$LLR_{APP_q} = \log\left(\frac{P(b_q=1|Y)}{P(b_q=0|Y)}\right) = \log\left(\frac{P(Y|b_q=1)P(Y)}{P(Y|b_q=0)P(Y)}\right) = \log\left(\frac{P(Y|b_q=1)}{P(Y|b_q=0)}\right) \tag{4}$$

Let's now define $x_j, 1 \leq j \leq 2^{M-1}$ as a transmitted symbol, such that $b_q = 1$, and $x_t, 1 \leq t \leq 2^{M-1}$ as a transmitted symbol, such that $b_q = 0$, then:

$$P(Y|b_q=1) = \sum_{\forall j} P(Y|x_j)P(x_j) \tag{5}$$

$$P(Y|b_q=0) = \sum_{\forall t} P(Y|x_t)P(x_t) \tag{6}$$

Now, considering equation (2),

$$P(Y|x_j) = \prod_{i=1}^{N} \frac{1}{\sqrt{2\pi\sigma^2}} e^{-\frac{\left(y_i - c_{i,x_j}\right)^2}{2\sigma^2}} = \frac{1}{\left(2\pi\sigma^2\right)^{\frac{N}{2}}} e^{-\frac{1}{2\sigma^2}\sum_{i=1}^{N}\left(y_i^2 + c_{i,x_j}^2\right) + \frac{1}{\sigma^2}\sum_{i=1}^{N} y_i c_{i,x_j}} \tag{7}$$

$$P(Y|x_t) = \prod_{i=1}^{N} \frac{1}{\sqrt{2\pi\sigma^2}} e^{-\frac{\left(y_i - c_{i,x_t}\right)^2}{2\sigma^2}} = \frac{1}{\left(2\pi\sigma^2\right)^{\frac{N}{2}}} e^{-\frac{1}{2\sigma^2}\sum_{i=1}^{N}\left(y_i^2 + c_{i,x_t}^2\right) + \frac{1}{\sigma^2}\sum_{i=1}^{N} y_i c_{i,x_t}} \tag{8}$$

where c_{i,x_j} corresponds with the ith chip of the PRN sequence associated to the symbol x_j and c_{i,x_t} correspondwith the ith chip of the PRN sequence associated to the symbol x_t. Remark that $c_{i,x_j} \in (1,-1)$ and $c_{i,x_t} \in (1,-1)$, then $c_{i,x_j}^2 = 1$ and $c_{i,x_t}^2 = 1$, yielding equation (4) to:

$$LLR_{APP_q} = \log\left(\frac{\sum_{\forall j} e^{\frac{1}{\sigma^2}\sum_{i=1}^{N} y_i c_{i,x_j}} P(x_j)}{\sum_{\forall t} e^{\frac{1}{\sigma^2}\sum_{i=1}^{N} y_i c_{i,x_t}} P(x_t)}\right) \tag{9}$$

Considering that the qth bit of the symbol x_j is always equal to 1 and the qth bit of the symbol x_t is always equal to 0, then equation (9) yields to:

$$\begin{aligned} LLR_{APP_q} &= \log\left(\frac{\sum_{\forall j}\left(e^{\frac{1}{\sigma^2}\sum_{i=1}^{N} y_i c_{i,x_j}} P(b_q=1)\prod_{z\neq q} P(b_{j,z})\right)}{\sum_{\forall t}\left(e^{\frac{1}{\sigma^2}\sum_{i=1}^{N} y_i c_{i,x_t}} P(b_q=0)\prod_{z\neq q} P(b_{t,z})\right)}\right) \\ &= \log\left(\frac{P(b_q=1)\sum_{\forall j}\left(e^{\frac{1}{\sigma^2}\sum_{i=1}^{N} y_i c_{i,x_j}} \prod_{z\neq q} P(b_{j,z})\right)}{P(b_q=0)\sum_{\forall t}\left(e^{\frac{1}{\sigma^2}\sum_{i=1}^{N} y_i c_{i,x_t}} \prod_{z\neq q} P(b_{t,z})\right)}\right) \end{aligned} \tag{10}$$

where $b_{j,z}$ is the zth bit of the transmitted symbol x_j and $b_{t,z}$ is the zth bit of the transmitted symbol x_t.

Applying the logarithm properties, equation (10) yields to:

$$LLR_{APP_q} = \log\left(\frac{\sum_{\forall j}\left(e^{\frac{1}{\sigma^2}\sum_{i=1}^{N} y_i c_{i,x_j}} \prod_{z\neq q} P(x_{j,z})\right)}{\sum_{\forall t}\left(e^{\frac{1}{\sigma^2}\sum_{i=1}^{N} y_i c_{i,x_t}} \prod_{z\neq q} P(x_{t,z})\right)}\right) + \log\left(\frac{P(b_q=1)}{P(b_q=0)}\right) \tag{11}$$

Remark that the term $\sum_{i=1}^{N} y_i c_{i,x_j}$ correspond with the correlation operation between the emitted and the received PRN sequences. Furthermore, from equation (11), LLR_{APP_q} can be divided in two different LLRs:

$$LLR_{APP_q} = LLR_{e,q} + LLR_{a,q} \tag{12}$$

- The extrinsic LLR LLR_e, which represents the information provided by the demodulation process.
- The a-priori LLR LLR_a, which represents the a priori information.

$$LLR_{a,q} = \log\left(\frac{P(b_q=1)}{P(b_q=0)}\right) \tag{13}$$

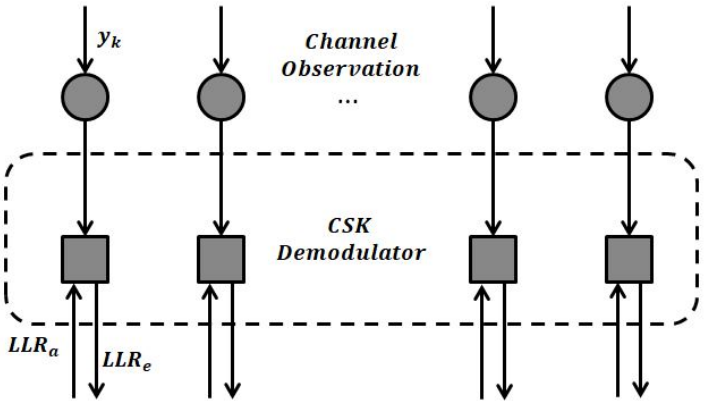

Figure 2: CSK Demodulator

In figure 2, it is illustrated the CSK demodulator. Remark that LLR_e is sent to the Root Protograph LDPC decoder and LLR_a is provided as the extrinsic information of the Root Protograph LDPC decoder.

Considering the precedent:

1. When the CSK demodulator is only fed by the channel observation and no a priori information is provided by the Root Protograph LDPC decoder, the CSK demodulator considers equiprobable bits and $LLR_a = 0$. This scheme is denoted **BICM**.

2. When the CSK demodulator is fed by the channel observation and the LLR_a provided by the Root Protograph LDPC decoder, the CSK demodulator considers equiprobable bits only in the first iteration. This scheme is denoted **BICM-ID**.

III-ROOT PROTOGRAPH LDPC CODES

We now investigate on Root LDPC codes. These codes belong to a family of codes having both MDS and full diversity properties under iterative BP decoding algorithm and they have been initially introduced for the block fading channel [2].

The non-ergodic block-fading channel [2] is a simplified channel model that characterizes slowly-varying fading channels. It can be viewed as an extension of the well-known block-erasure channel which considers that some parts of the message are completely erased due to a deep fade of the channel or, because of the lack of received data. Under this context, a transmitted codeword can be viewed as finite number n_c of independent channel realizations.

We consider a block-fading channel with n_c fading blocks, whose discrete-time channel output at time i is given by:

$$y_i = h_i x_i + z_i, i = 1, \ldots, N_f \tag{14}$$

where N_f denotes the frame length, $x_i \in \{-1, +1\}$ is the $i-th$ binary phase shift keying (BPSK) modulated symbol, $z_i \sim \mathcal{N}(0, \sigma^2)$ are the centered *i.i.d.* Gaussian noise samples with variance $\sigma^2 = N_0/2$, and h_i is a real fading coefficient that belongs to the set $\mathbb{N} = \{\alpha_1, \alpha_2, \ldots, \alpha_{nc}\}$. Figure 3 illustrates a codeword under the block fading channel scenario.

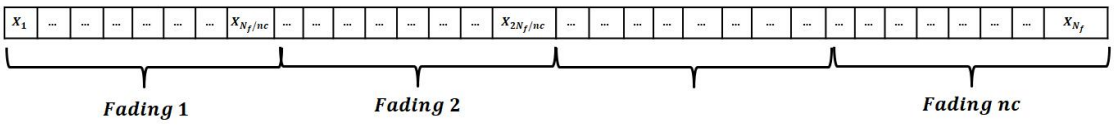

Figure 3: Message Structure

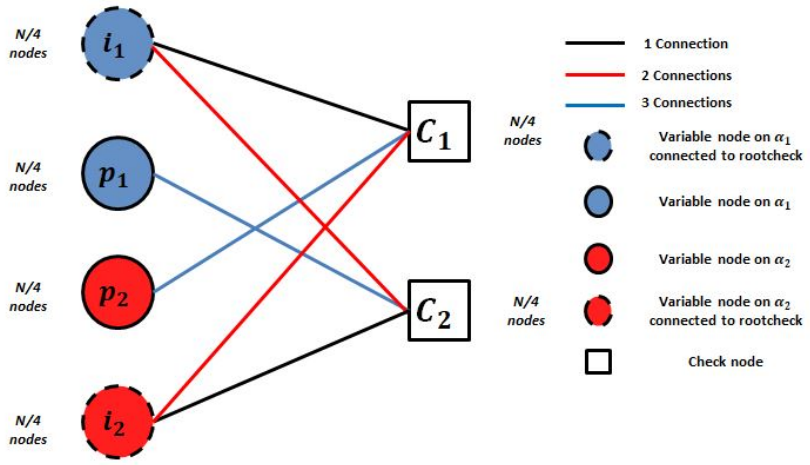

Figure 4: Tanner Graph for a Regular (3,6) Root LDPC Code of Rate 1/2

The design of the Root LDPC codes has roots in the limiting case where the fading coefficient can belong to $\mathbb{N} \in \{0, 1\}$, which corresponds to the well-known block erasure channel [6]. Indeed, as it was shown in [2], the usual single parity check nodes involved in LDPC codes is not sufficient to tolerate more than one erasure bit. Therefore, a new check node structure, referred to as rootcheck node, is introduced, enabling more than one erasure bit under the BP decoding algorithm.

Considering the precedent, the construction of the regular Root LDPC code is presented for a block fading channel $nc = 2$.

Definition 1. [2] Let x_1 be a binary element transmitted on fading α_1. A rootcheck for x_1 is a checknode $\Phi(x_1, x_2, \ldots, x_\delta)$ where all bits $x_2, \ldots, x_\delta$ are transmitted on fading α_2.

Using Definition 1, the design of a length-N rate-1/2 systematic regular LDPC code that has to operate on a two-blocks fading channel can be summarized as follows. Two classes of bits are first defined, i.e. systematic information bits and redundant parity bits. The $N/2$ systematic information bits are split into two classes: $N/4$ bits (noted i_1), which are transmitted on the block with fading α_1 and $N/4$ bits (noted i_2), which are transmitted on the block with fading α_2. Parity bits are also partitioned into two sets (noted p_1 and p_2 respectively) and sent to the channel following the same assumptions as for the information bits. This mapping of the information and redundant/parity bits is represented in Figure 4 using the bipartite Tanner protograph representation that also shows how the different information and parity bits are connected to rootchecks.

The corresponding block structure of the associated parity check matrix H is directly derived from its Tanner protograph and is given in equation (15) by

$$H_\beta = \begin{bmatrix} I & 0 & H_{i_2} & H_{p_2} \\ H_{i_1} & H_{p_1} & I & 0 \end{bmatrix}, \tag{15}$$

where I and 0 are $N/4 \times N/4$ identity and all-zero matrices respectively. H_{i_k} and H_{p_k}, $k \in (1, 2)$, are sparse regular matrices of Hamming weight 2 and 3 per row and per column respectively. Examining equation (15), under the block-erasure channel scenario, we observe that the only outage event occurs when $\alpha_1 = \alpha_2 = 0$ (both blocks erased). Indeed, when $\alpha_1 = 0$ and $\alpha_2 = 1$, it is straightforward to see that information bits i_1 are determined using rootchecks c_1. Similarly, when $\alpha_1 = 1$ and $\alpha_2 = 0$, information bits i_2 are determined using rootchecks c_2. Considering the precedent let ϵ be the probability that $\alpha_i, i = 1, 2$, be equal to zero. Then the word error probability of the Root LDPC code is ϵ^2, which precisely the outage probability of the block erasure channel [6]. Therefore the Root LDPC code are outage achieving in the block erasure channel and as a consequence full diversity.

Remark that the Root LDPC codes are outage achieving in the block erasure channel but that it not a sufficient condition to have the full diversity property in noisy channels. Therefore, in [2], it is presented the behavior of the Root LDPC codes over general Rayleigh block fading AWGN channel, providing that those codes are also full diversity over this channel.

From Definition 1, it is trivial that the data structure of a regular Root LDPC (3,6) code must be divided into two different blocks, each one corresponding to α_1 or α_2. Once one of the blocks is received, the decoding process starts by executing the BP algorithm. In case of retrieving a correct CRC the CED is retrieved, otherwise another block must be received.

Root as Protograph Structure

Considering the parity check matrix H in equation (15), Let us now introduce the so-called base matrix H_B associated with the protograph of the regular Root LDPC code given by equation (15). The base matrix H_B is given by

$$H_B = \begin{bmatrix} 1 & 0 & 2 & 3 \\ 2 & 3 & 1 & 0 \end{bmatrix}. \tag{16}$$

In this representation, the coefficient $H_B(i,j)$ represents the number of connections/edges between variable nodes of type i with check nodes of type j. Thus, for the regular Root LDPC code, we have 4 types of variable nodes noted (i_1, p_1, i_2, p_2) and two types of check nodes noted (c_1, c_2). Thus, for example, the variable nodes of type i_1 are connected to one check node of type c_1 and two check nodes of type c_2.

Remark that a protograph is a Tanner graph G for which parallel edges are permitted. In order to generate a LDPC code from a protograph, a *copy and permute* operation also called lifting is used to interleave multiple copys of the original protograph [18]. LDPC codes generated from protographs can enhance the error correcting performance compared to Regular LDPC codes, since good irregular LDPC codes can be designed.

The protograph LDPC codes, that are optimized in sections IV and V, are irregular structures. To do so, we adopt the following general protograph representation for a Root LDPC code of rate $R = 1/2$:

$$H_B = \begin{bmatrix} 1 & 0 & * & * \\ * & * & 0 & 1 \end{bmatrix} \tag{17}$$

where $*$ represents connection weights $\in \mathbb{N}$ to be optimized. In [4], some optimized structure have been presented considering the Protograph structure in equation (17), however small gains in the demodulation threshold with respect to the regular Root LDPC codes has been observed. To enhance the demodulation threshold gains, [4] rather considered the following lifted protograph representation :

$$H_{\beta_1} = \begin{bmatrix} 1 & 0 & 0 & 0 & * & * & * & * \\ 0 & 1 & 0 & 0 & * & * & * & * \\ * & * & * & * & 1 & 0 & 0 & 0 \\ * & * & * & * & 0 & 1 & 0 & 0 \end{bmatrix} \tag{18}$$

This structure also presents the Root LPDC connections and it provides more number of degree of freedom in order to optimize the demodulation threshold.

Root Protograph LDPC Decoding Scheme

As it was already presented in [12], the Root Protograph structure must be divided into two different blocks, each one corresponding to α_1 or α_2. Once one of the blocks is received, the decoding process starts by executing the BP algorithm under the **BICM** scheme or by exectuing the iterative decoding between the CSK demodulator and the BP algorithm under the **BICM-ID** scheme. In case of retrieving a correct CRC the CED is retrieved, otherwise another block must be received. The decoding scheme is described in Figure 5.

In the following sections, we provide the methods to optimized the Root Protograph structure with $n_c = 2$, considering that the CSK modulated signal in a BICM context and a CSK modulated signal in a BICM-ID context.

IV OPTIMIZATION OF THE PROTOGRAPH LDPC CODES FOR A CSK MODULATION SIGNAL IN A BICM CONTEXT

Let's consider the definition of the Protograph graph $G = (N, M, E)$ in [18] with N the number of variable nodes, M the number of check nodes and E the set of edges, we define the variable node $v_j, j = 1, \ldots, N$, the check node $c_i, i = 1, \ldots, M$ and the edges $b_{i,j}$.

Considering the precedent, we present the following mutual information definitions:

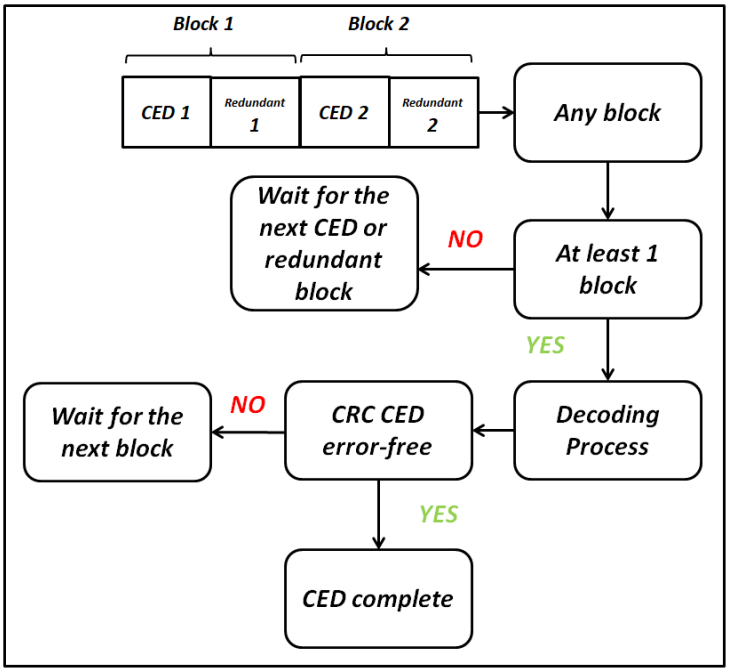

Figure 5: Root-LDPC Decoding Scheme

- $I_{Av}(i,j)$ denotes the a-priori mutual information between the input LLR of v_j on each of the $b_{i,j}$ edges and the corresponding codeword bit v_j.
- $I_{Ac}(i,j)$ denotes the a-priori mutual information between the input LLR of c_i on each of the $b_{i,j}$ edges and the corresponding coded bit v_j.
- $I_{Ev}(i,j)$ denotes the extrinsic mutual information between the sent LLR by v_j to c_i and the corresponding codeword bit v_j.
- $I_{Ec}(i,j)$ denotes the extrinsic mutual information between the sent LLR by c_i to v_j and the corresponding codeword bit v_j.
- $I_{APP}(j)$ denotes the a-posteriori mutual information between the a-posteriori LLR of and the corresponding codeword bit v_j.

Now, considering the CSK demodulator in figure 2, we can compute the mutual information at the input of the Root Protograph LDPC decoder. In figure 6 it is illustrated the CSK demodulator and the Protograph LDPC decoder considering a BICM scheme.

Remark that under AWGN channel, we denote I_{Ch} as the channel mutual information at the input of the CSK demodulator. Considering that the CSK demodulator is not fed by the a-priori mutual information provided by the Root Protograph decoder, the extrinsic mutual information provided by the CSK demodulator I_E is constant for each of the Protograph variable nodes.

Considering the precedent, we can use the Protograph Exit Chart algorithm over the AWGN channel in order to optimize the Protograph structure.

Applying the precedent algorithm, we have obtained the following optimized Protograph:

$$H_{\beta_1} = \begin{bmatrix} 1 & 0 & 0 & 0 & 2 & 1 & 3 & 0 \\ 0 & 1 & 0 & 0 & 2 & 0 & 3 & 1 \\ 1 & 3 & 0 & 2 & 1 & 0 & 0 & 0 \\ 0 & 3 & 2 & 1 & 0 & 1 & 0 & 0 \end{bmatrix} \tag{19}$$

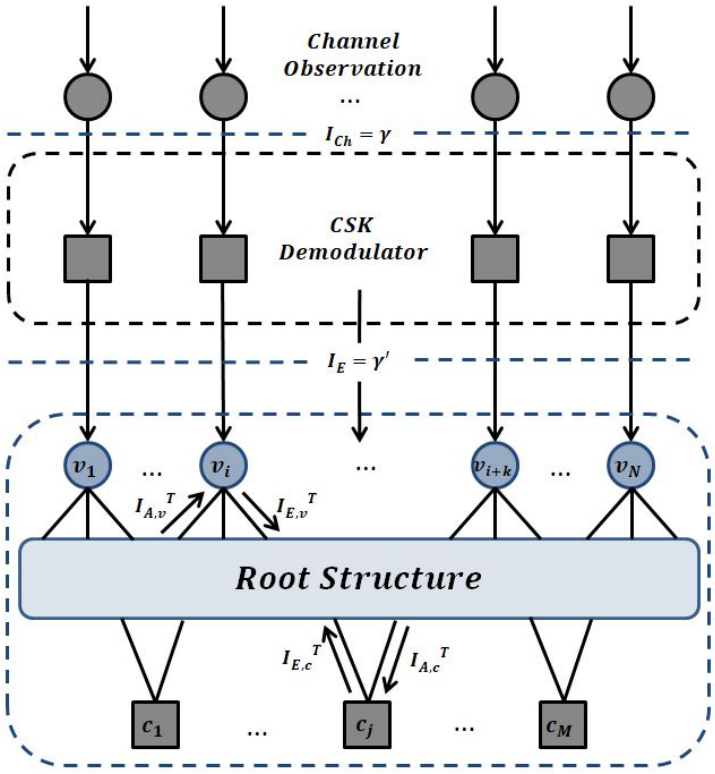

Figure 6: CSK Demodulator and Protograph LDPC decoder considering a BICM scheme

Remark from the precedent that since this method does not turbo iterate with the CSK demodulator, the Optimized Protograph structure is independent from the CSK modulation order.

V OPTIMIZATION OF THE PROTOGRAPH LDPC CODES FOR A CSK MODULATION SIGNAL IN A BICM-ID CONTEXT

Considering the mutual information definitions for a Protograph structure in section IV and the CSK demodulator in figure 2. In figure 7 it is illustrated the CSK demodulator and the Root Protograph LDPC decoder considering a BICM-ID scheme.

Remark that under AWGN channel, we denote I_{Ch} as the channel mutual information at the input of the CSK demodulator. Considering that the CSK demodulator is fed by the channel observation and the a-priori mutual information provided by the Root Protograph decoder $I_{A\_CSK}(q)$, the extrinsic mutual information provided by the CSK demodulator $I_{E\_CSK}(q)$ changes in each iteration and varies from one Protograph variable node to another.

EXIT Charts for CSK modulation in AWGN Channel

In this section, we present an asymptotic analysis via EXtrinsic Information Transfer (EXIT) charts [16] in AWGN channel, to show that bit interleaved iterative decoding for a CSK modulated signal (consisting in adding a soft feedback between the LDPC decoder and the soft CSK demodulator) can significantly outperform non-iterative decoding.

The EXIT Chart is a graphical tool which represents the extrinsic mutual information I_e between the sent bits and the extrinsic LLRs at the output of a soft input soft output block, as a function a-priori mutual information I_a between the sent bits and the a-priori LLRs at the input of a soft input soft output block

Considering the results in section II, let's denote $I_{a,q}$ as the mutual information between the qth bit b_q of the emitted CSK PRN sequence and the a-priori message $LLR_{a,q}$. Considering a binary input memoryless channel, $I_{a,q}$

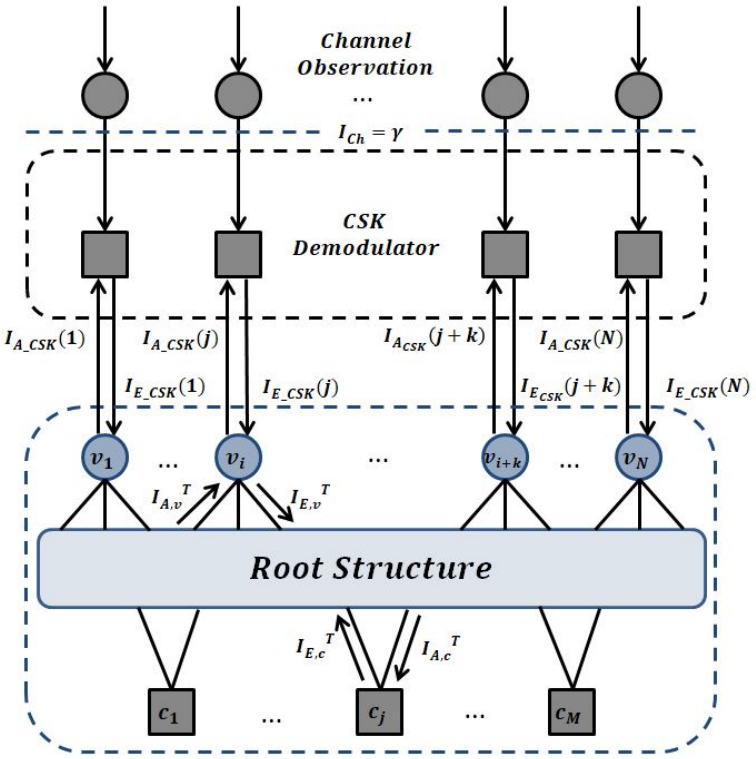

Figure 7: CSK Demodulator and Protograph LDPC decoder considering a BICM-Id scheme

can be generally defined as [14]:

$$I_{a,q} = \frac{1}{2} \sum_{b_q \pm 1} \int_{-\infty}^{+\infty} P(LLR_{a,q}|b_q) log_2 \left(\frac{2P(LLR_{a,q}|b_q)}{P(LLR_{a,q}|b_q = +1) + P(LLR_{a,q}|b_q = -1)} \right) dLLR_{a,q} \tag{20}$$

Equation (20) can be simplified by:

$$I_{a,q} = 1 - \int_{-\infty}^{+\infty} log_2 \left(1 + e^{-LLR_{a,q}}\right) P(LLR_{a,q}|b_q = +1) dLLR_{a,q} \tag{21}$$

if $LLR_{a,q}|b_q$ can be generated assuming the consistent Gaussian approximation [14]:

- $P(LLR_{a,q})$ follow a Gaussian distribution with σ_a as its standard deviation and μ_a as its means.
- $P(LLR_{a,q})$ is exponential consistent [14], then $\sigma_a^2 = 2\mu_a$

Considering the precedent:

$$I_{a,q} = 1 - \int_{-\infty}^{+\infty} log_2 \left(1 + e^{-LLR_{a,q}}\right) \frac{1}{2\pi\sigma_a^2} e^{-\frac{\left(LLR_{a,q} - \frac{\sigma_a^2}{2}\right)^2}{2\sigma_a^2}} dLLR_{a,q} = J(\sqrt{\sigma_a^2}). \tag{22}$$

where $J(\sigma)$ represents the input-output mutual information of the channel [8], then,

$$\sigma_a^2 = J^{-1}(I_{a,q}) \tag{23}$$

and consequently:

$$LLR_{a,q}|b_q = \pm 1 \sim \mathcal{N}\left(\pm\frac{\sigma_a^2}{2}, \sigma_a^2\right) \tag{24}$$

In order to compute $J(\sigma)$ and the inverse $J(\cdot)^{-1}$, polynomial approximation were presented in [17].

Once the a-priori $LLR_{a,q}|b_q$ are precomputed, the CSK signal under AWGN channel is simulated to compute the CSK demodulator output LLR_{APP_q} as in equation 11.

Then $LLR_{e,q}$ are deduced from the LLR_{APP_q} values through equation 12.

Finally, the extrinsic mutual information $I_{e,q}$ can be computed as:

$$I_{e,q} = \frac{1}{2}\sum_{b_q \pm 1}\int_{-\infty}^{+\infty} P(LLR_{e,q}|b_q) log_2\left(\frac{2P(LLR_{e,q}|b_q)}{P(LLR_{e,q}|b_q=+1)+P(LLR_{e,q}|b_q=-1)}\right) dLLR_{e,q} \tag{25}$$

The above expression can be well evaluated though a Monte-Carlo simulation estimation using histogram [13].

Considering the CSK demodulator, in figure 7 $I_{a,q}$ and $I_{e,q}$ are denoted as $I_{A\_CSK}(q)$ and $I_{E\_CSK}(q)$.

In figure 8, it is illustrated $I_{A\_CSK}(q)$ and $I_{E\_CSK}(q)$ for different modulation order once one Es/N_0 is set. Moreover, in figure 9, it is illustrated $I_{A\_CSK}(q)$ and $I_{E\_CSK}(q)$ for different Es/N_0, given a modulation order $M = 6$.

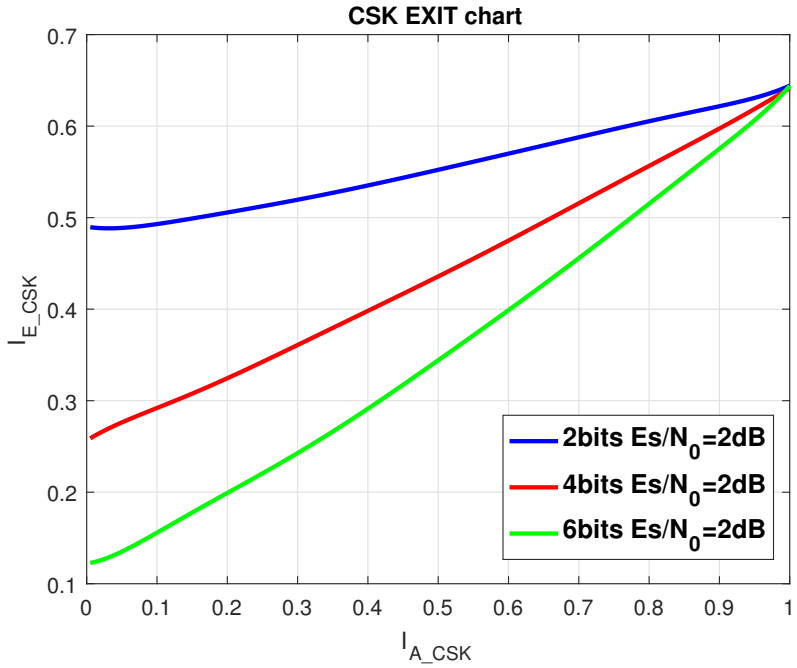

Figure 8: CSK EXIT charts for different CSK modulation order/ $Es/N_0 = 2dB$

Considering the precedent, given a the set value I_{Ch}, we can compute the extrinsic mutual information $I_{e,q} \in [0,1]$ given the a a-priori mutual information value $I_{a,q} \in [0,1]$.

Then, we can apply a modified version of the Protograph EXIT chart algorithm which considers the iterative decoding between the CSK demodulator and the LPCD decoder. In this paper, we have computed the optimal Protograph structures considering different CSK modulation orders ($M = 2$, $M = 4$ and $M = 6$). The structures are the following:

- 2ary CSK modulation

$$H_{M=2} = \begin{bmatrix} 1 & 0 & 0 & 0 & 3 & 1 & 2 & 0 \\ 0 & 1 & 0 & 0 & 3 & 0 & 1 & 1 \\ 1 & 0 & 0 & 3 & 1 & 0 & 0 & 0 \\ 0 & 3 & 2 & 1 & 0 & 1 & 0 & 0 \end{bmatrix} \tag{26}$$

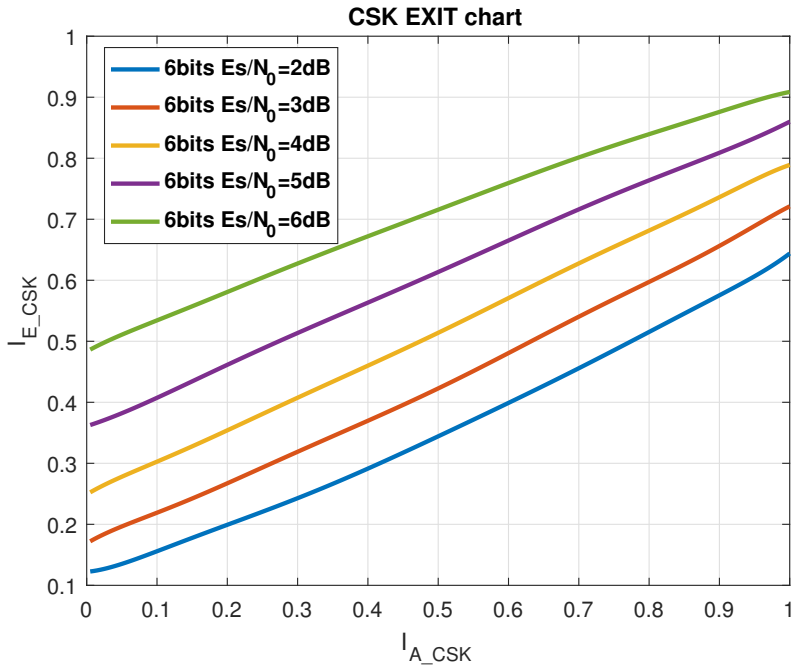

Figure 9: CSK EXIT charts for different Es/N_0 / CSK modulation order $M = 6$

- 4ary CSK modulation

$$H_{M=4} = \begin{bmatrix} 1 & 0 & 0 & 0 & 0 & 1 & 2 & 1 \\ 0 & 1 & 0 & 0 & 1 & 0 & 2 & 0 \\ 1 & 3 & 1 & 2 & 1 & 0 & 0 & 0 \\ 0 & 1 & 3 & 0 & 0 & 1 & 0 & 0 \end{bmatrix} \tag{27}$$

- 6ary CSK modulation

$$H_{M=6} = \begin{bmatrix} 1 & 0 & 0 & 0 & 0 & 1 & 2 & 0 \\ 0 & 1 & 0 & 0 & 1 & 0 & 1 & 1 \\ 1 & 3 & 2 & 3 & 1 & 0 & 0 & 0 \\ 0 & 1 & 2 & 0 & 0 & 1 & 0 & 0 \end{bmatrix} \tag{28}$$

RESULTS

For both schemes, finite length Quasi-Cyclic (QC) parity-check matrices [7] have been generated. Results related to the BICM scheme are illustrated in figures 10, 11 and 12. Figure 10 illustrates the error correcting performance of the LDPC code constructed using the protograph (19) for CSK modulation orders $M = 2$, $M = 4$ and $M = 6$. This figure also illustrates the error correcting performance of the GPS L1C subframe 2 LDPC code for CSK modulation orders $M = 2$, $M = 4$ and $M = 6$. We can remark that for order $M = 2$, the protograph code performs as the GPS code. However, for higher orders of modulation, we can notice that the error correcting capabilities of the proposed Protograph code are better than those of the GPS L1C subframe 2 code.

In [10], the fact that root codes can reduce the TTD was shown via Cumulative Distribution Function (CDF) of the TTD. This improvement has been achieved because the initially proposed coding scheme took into account the structure of the message. In this article, we present a new method to show that root codes can reduce the TTD without considering the message structure. The idea is to compute the error correcting capability of each code, when a given percentage of the message is retrieved and considering that the first acquired symbol can be in different parts of the message. For instance, figures 11 and 12 provide the error correction capabilities of the GPS L1C subframe

LDPC code [1] and the proposed Root Protograph (19) code for a CSK modulation of order $M = 2$ and different E_b/N_0, when $x_i = 1$, $x_i = N/4$, $x_i = N/2$ and $x_i = 3N/2$. Note that x_i is the first acquired symbol and N is the size of the codeword. Considering the FER for a $Eb/N_0 = 3.4dB$, the Root Protograph code provides better error correcting capabilities comparing to the GPS L1C subframe 2 code, when $x_i = 1$, $x_i = N/4$ and $x_i = N/2$. When consider the FER for a $Eb/N_0 = 10dB$ (High SNR), the Root Protograph code provides better error correcting capabilities comparing to the GPS L1C subframe 2 code; independently of x_i. We remark under this case that GPS L1C subframe 2 code finds hard to converge when $x_i = N/2$.

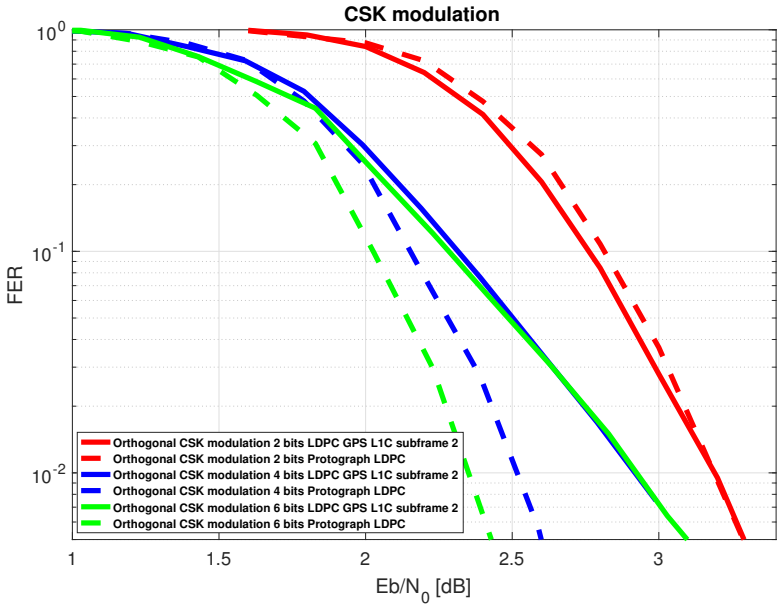

Figure 10: FER: GPS L1C subframe 2 code vs Protograph code under BICM scheme

In figures 13, 14, 15, 16, 17 and 18, we present the results of the error correction capabilities under BICM-ID scheme for CSK modulation orders $M = 2$, $M = 4$ and $M = 6$.

In figure 14 and 13 we provide the result of Frame Error Rate (FER) and Bit Error Rate (BER) for a the Protograph Root code optimized for a $M = 2$ CSK modulation. We compare the previous code with a $M = 2$ CSK modulation encoded with the GPS L1C subframe 2 LDPC code. Simulation results show an improvement of 0.2 dB for a FER of 10^{-2} and 0.3 dB for a BER of 10^{-3}. Moreover, we remark that the BICM-ID scheme provides an improvement around 0.7 dB with respect to the BICM scheme for an FER 10^{-2} and an improvement around 0.6 dB for a BER of 10^{-3}.

In figure 16 and 15 we provide the result of Frame Error Rate (FER) and Bit Error Rate (BER) for a the Protograph Root code optimized for a $M = 4$ CSK modulation. We compare the previous code with a $M = 4$ CSK modulation encoded with the GPS L1C subframe 2 LDPC code. Simulation results show an improvement of 0.4 dB for a FER of 10^{-2} and 0.4 dB for a BER of 10^{-3}. Moreover, we remark that the BICM-ID scheme provides an improvement around 1.8 dB with respect to the BICM scheme for an FER 10^{-2} and an improvement around 1.2 dB for a BER of 10^{-3}.

In figure 18 and 17 we provide the result of Frame Error Rate (FER) and Bit Error Rate (BER) for a the Protograph Root code optimized for a $M = 6$ CSK modulation. We compare the previous code with a $M = 6$ CSK modulation encoded with the GPS L1C subframe 2 LDPC code. Simulation results show an improvement of 0.5 dB for a FER of 10^{-2} and 0.6 dB for a BER of 10^{-3}. Moreover, we remark that the BICM-ID scheme provides an improvement around 2 dB with respect to the BICM scheme for an FER 10^{-2} and an improvement around 1.4 dB for a BER of 10^{-3}.

As a future work, it is expected to simulate both scheme considering the decoding scheme in figure 5, showing the reduction of the TTD via CDF over different types of scenarios (AWGN channel with High a low C/N_0, LMS channel, ...).

CONCLUSIONS

In this article, we proposed two new channel code designs for protograph root codes in the context of both **BICM** and **BICM-ID** schemes and that are optimized for the CSK modulation with order $M = 2$, $M = 4$ and $M = 6$ (the methodology can be applied for higher CSK orders). These codes are characterized by the MDS property which allows for a reduction of the TTD. We first provide the results considering the **BICM** scheme, showing that the proposed Protograph structure performs better than the GPS L1C subframe 2 irregular LDPC code under AWGN channel, considering CSK orders $M > 2$. Futhermore, in this paper it is also provide a new method to verify the potential of the MDS a full diversity property considering the the burst erasure channel. Simulation results shown interesting results in terms of error correction capabilities. Secondly, we provide the results considering the **BICM-ID** scheme. Simulation results illustrated that the optimized Protograph structure improve those results provide by the GPS L1C subframe 2 irregular LDPC code. As a future work, It is expected to simulate the entire decoding scheme, providing results of the TTD via CDF over different types of scenarios.

ACKNOWLEDGEMENTS

This work is funded by the French Space Agency, CNES, and Thales Alenia Space.

REFERENCES

[1] Interface Specification IS-GPS-800 NavStar GPS Space Segment / User Segment L1C Interface. Technical report.

[2] J. J. Boutros, A. G. i Fàbregas, E. Biglieri, and G. Zémor. Low-density parity-check codes for nonergodic block-fading channels. *IEEE Transactions on Information Theory*, 56(9):4286–4300, 2010.

[3] G. Caire, G. Taricco, and E. Biglieri. Bit-interleaved coded modulation. *IEEE Transactions on Information Theory*, 44(3):927–946, May 1998.

[4] Y. Fang, G. Bi, and Y. L. Guan. Design and analysis of root-protograph ldpc codes for non-ergodic block-fading channels. *IEEE Transactions on Wireless Communications*, 14(2):738–749, 2014.

[5] A. J. Garcia Peña, D. Salós, O. Julien, L. Ries, and T. Grelier. Analysis of the use of CSK for Future GNSS Signals. In *ION GNSS 2013, 26th International Technical Meeting of The Satellite Division of the Institute of Navigation*, pages pp 1461–1479, Nashville, United States, Sept. 2013. ION.

[6] A. G. i Fabregas and Q. Tang. Coding in the block-erasure channel. In *2006 Australian Communications Theory Workshop*, pages 19–24. IEEE, 2006.

[7] Y. Li and M. Salehi. Quasi-cyclic ldpc code design for block-fading channels. In *2010 44th Annual Conference on Information Sciences and Systems (CISS)*, pages 1–5, March 2010.

[8] G. Liva and M. Chiani. Protograph ldpc codes design based on exit analysis. In *IEEE GLOBECOM 2007 - IEEE Global Telecommunications Conference*, pages 3250–3254, Nov 2007.

[9] L. Ortega, C. Poulliat, M. Boucheret, M. Aubault, and H. AlBitar. Advanced co-design of message structure and channel coding scheme to reduce the time to ced and to improve the resilience for a galileo 2nd generation new signal. In *ESA Workshop on Satellite Navigation Technologies and European Workshop on GNSS Signals and Signal Processing (NAVITEC 2018), Noordwijk, The Netherlands, 05/12/2018-07/12/2018*.

[10] L. Ortega, C. Poulliat, M. Boucheret, M. Aubault, and H. AlBitar. Co-design of message structure and channel coding scheme to reduce the time to ced for a galileo 2nd generation new signal. In *Proceedings of the 31st International Technical Meeting of The Satellite Division of the Institute of Navigation (ION GNSS+ 2018), Miami, Florida, September 2018*, pages 4064–4078, 2018.

[11] L. Ortega, C. Poulliat, M. Boucheret, M. Aubault, and H. AlBitar. New solutions to reduce the time-to-ced and to improve the ced robustness of the galileo i/nav message. In *2018 IEEE/ION Position, Location and Navigation Symposium (PLANS)*, pages 1399–1408, April 2018.

[12] L. Ortega, C. Poulliat, M. Boucheret, M. Aubault, and H. AlBitar. Optimizing the Co-Design of Message Structure and Channel Coding to Reduce the TTD for a Galileo 2nd Generation Signal. *European Journal of Navigation*, (ARTICLE), 2019.

[13] M. Roudier. *Analysis and Improvement of GNSS Navigation Message Demodulation Performance in Urban Environments*. Theses, INP Toulouse, Jan. 2015.

[14] W. Ryan and S. Lin. *Channel Codes: Classical and Modern*. Cambridge University Press, 2009.

[15] A. M. O. M. B. T. Schotsch, Birgit E. Joint time-to-ced reduction and improvement of ced robustness in the galileo i/nav message. *Proceedings of the 30th International Technical Meeting of The Satellite Division of the Institute of Navigation (ION GNSS+ 2017), Portland, Oregon, September 2017*, pages 1544–1558.

[16] S. ten Brink. Convergence of iterative decoding. *Electronics Letters*, 35(10):806–808, May 1999.

[17] S. Ten Brink, G. Kramer, and A. Ashikhmin. Design of low-density parity-check codes for modulation and detection. *IEEE transactions on communications*, 52(4):670–678, 2004.

[18] J. Thorpe. Low-density parity-check (ldpc) codes constructed from protographs. 2003.

[19] A.-C. Wong and V. C. Leung. Code-phase-shift keying: a power and bandwidth efficient spread spectrum signaling technique for wireless local area network applications. In *CCECE'97. Canadian Conference on Electrical and Computer Engineering. Engineering Innovation: Voyage of Discovery. Conference Proceedings*, volume 2, pages 478–481. IEEE, 1997.

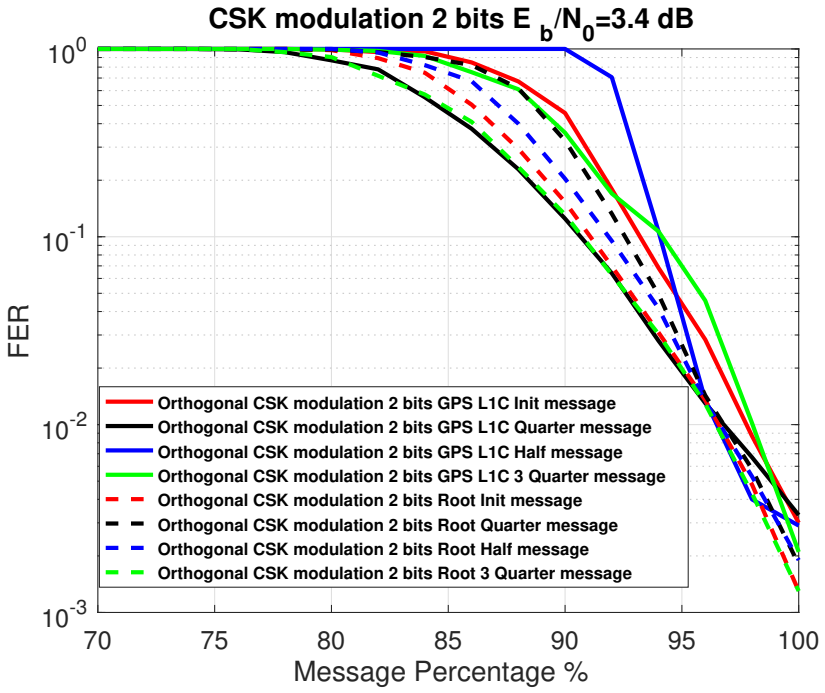

Figure 11: FER depending on the received percentage of the message, $\frac{E_b}{N_0} = 3.4dB$

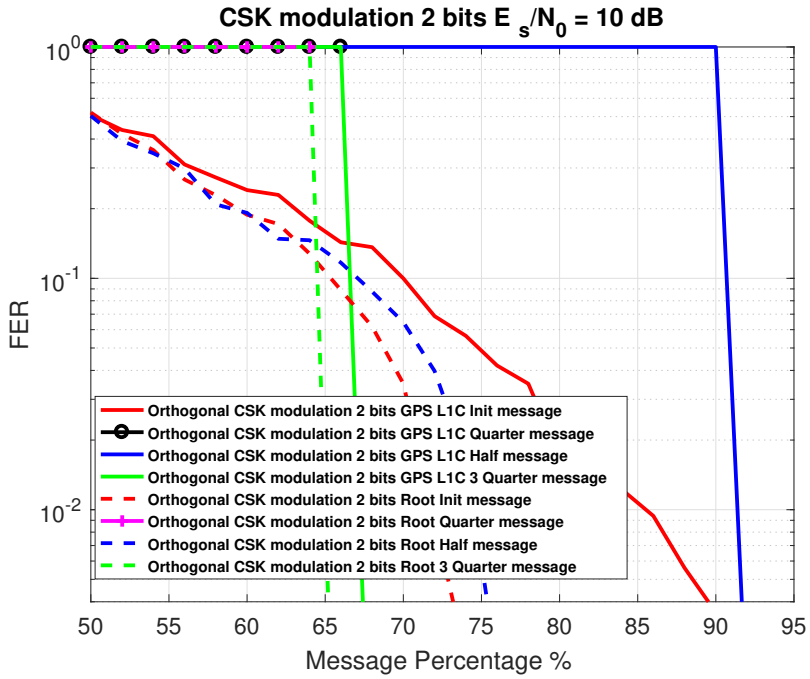

Figure 12: FER depending on the received percentage of the message, $\frac{E_b}{N_0} = 10dB$

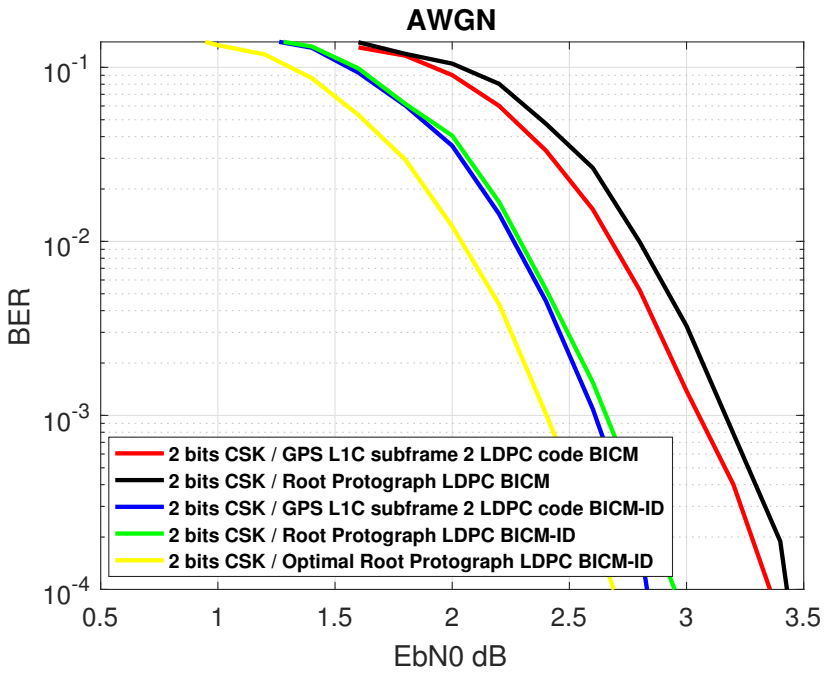

Figure 13: BER under BICM-ID scheme $M = 2$

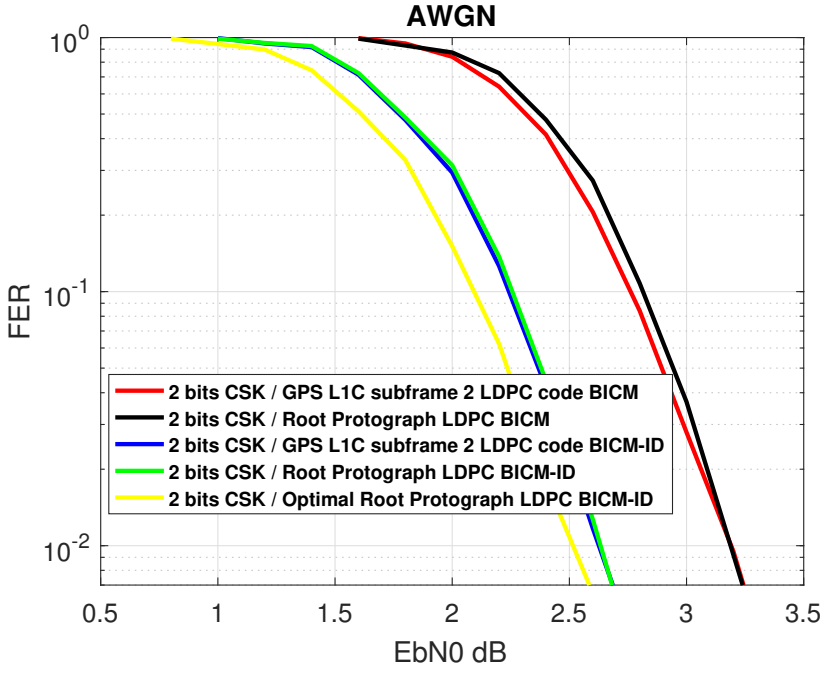

Figure 14: FER under BICM-ID scheme $M = 2$

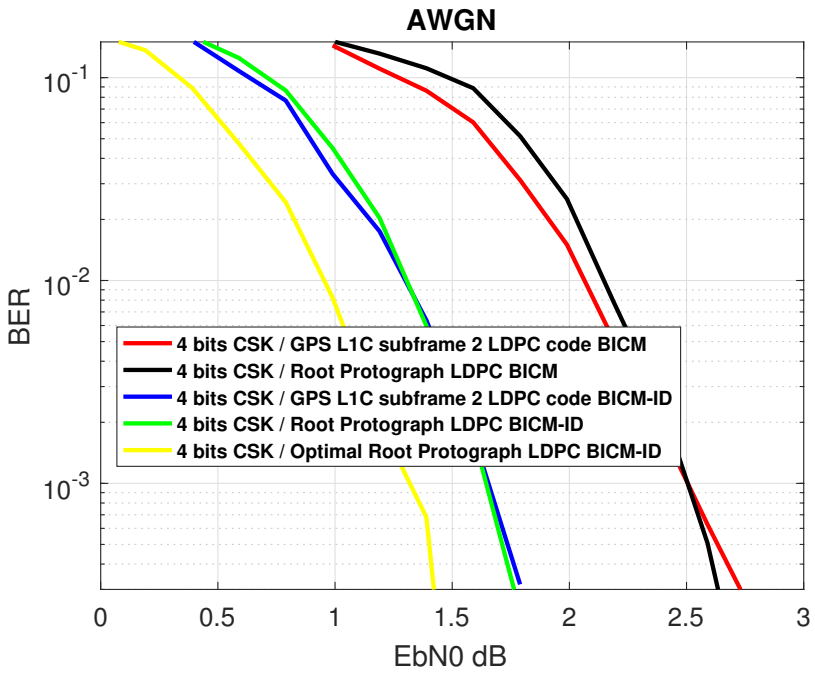

Figure 15: BER under BICM-ID scheme $M = 4$

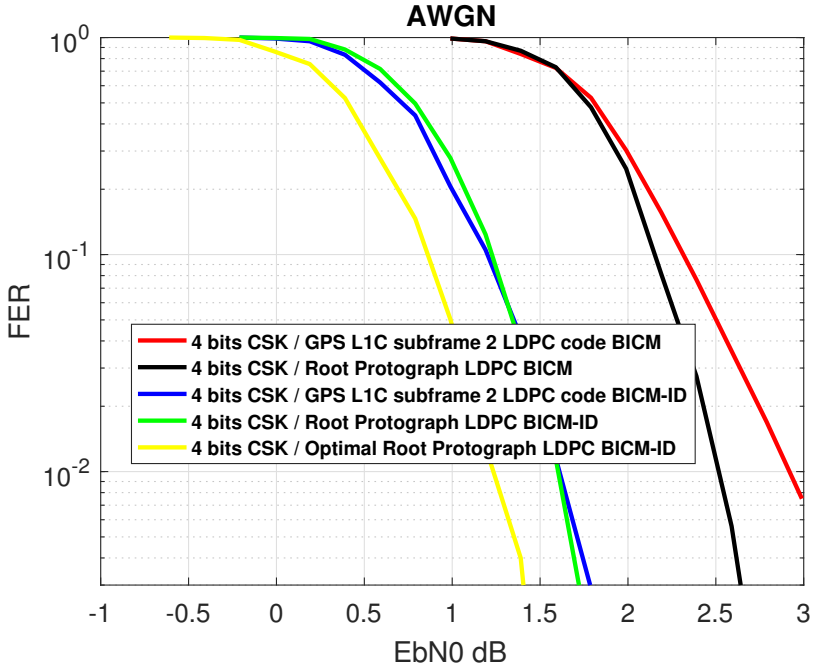

Figure 16: FER under BICM-ID scheme $M = 4$

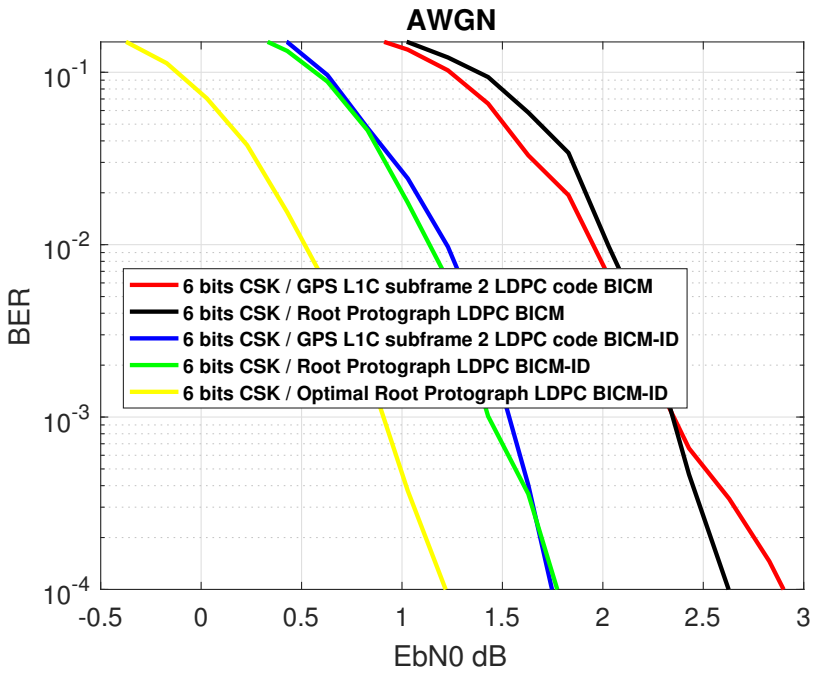

Figure 17: BER under BICM-ID scheme $M = 6$

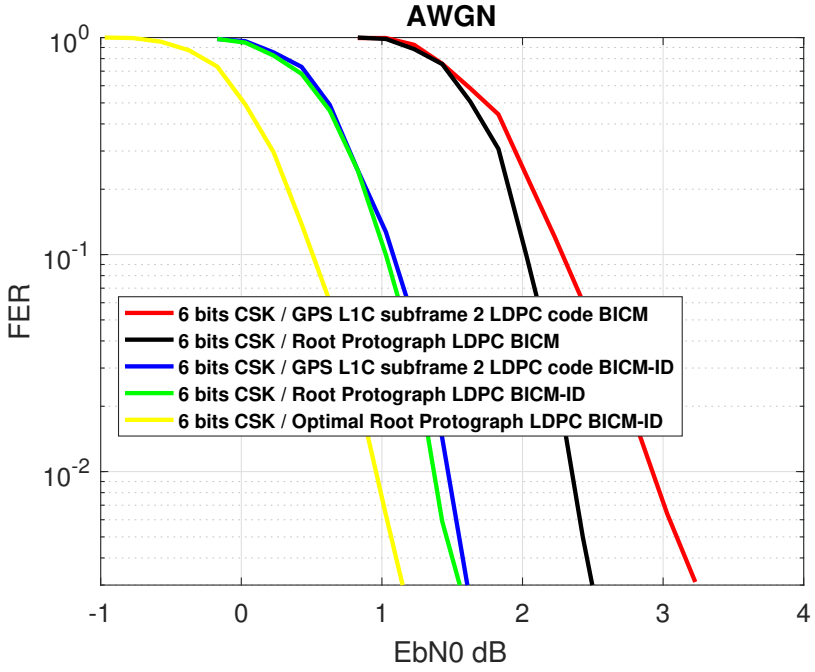

Figure 18: FER under BICM-ID scheme $M = 6$